

Absolute Gravity Variation at Sakurajima Volcano from April 2009 through January 2011 and its Relevance to the Eruptive Activity of Showa Crater

Shuhei OKUBO^{*}, Takahito KAZAMA^{*,**}, Keigo YAMAMOTO^{***}, Masato IGUCHI^{***},
Yoshiyuki TANAKA^{*}, Takayuki SUGANO^{*}, Yuichi IMANISHI^{*}, Wenke SUN^{*,****},
Mamoru SAKA^{*}, Atsushi WATANABE^{*} and Shigeo MATSUMOTO^{*****}

(Received September 30, 2011; Accepted February 27, 2012)

We describe absolute gravity measurements performed from April 2009 through January 2011, and present technical suggestions for carrying out continuous observations in a volcanic area. The results clearly show significant gravity variations of as large as 30 μgal during the observation period. Hydrological simulations reveal that about half of the gravity change is attributable to groundwater disturbance. After correcting for this disturbance, the observed variations in gravity can be divided into 5 separate phases. Phase I is a period with few eruptions, which extends from April to late June 2009 when an abrupt 10 μgal gravity decrease was observed. During the succeeding phase II, from July 2009 to May 2010, gravity oscillated about a mean value with an amplitude of 5 μgal , while the monthly number of explosions at Showa crater dramatically increased from 50 to about 150. In phase III, which was a transient quiescent period, gravity increased by as much as 10 μgal in a single month. This was followed by phase IV, during which there was a steady gravity decrease until November 2010. During the final phase V, gravity remained almost constant until at least January 2011. These five phases are closely linked to the eruptive activity at Showa crater. In fact, excellent correlations are found among the records of absolute gravity, ejected weight of volcanic ash, ground tilt, and infrasound air shock amplitude. The gravity data are transformed into changes in magma head height using a simplified line mass model.

Key words: absolute gravity, magma head, open conduit, Sakurajima volcano, Showa crater

1. Introduction

Sakurajima volcano woke from a decade-long period of dormancy in 2006. Many Vulcanian eruptions and pyroclastic flows from Showa crater have been recorded (Iguchi *et al.*, 2010). The volcanic activity since 2006, and in particular since 2009, exhibited the following features:

(1) Most of the eruptions occurred at Showa crater with only a few exceptions at Minamidake crater, which had been the major vent for a 50 year period since 1955.

(2) The annual number of explosive eruptions in 2010 marked the highest ever recorded in Sakurajima volcano since 1955. Roughly 500 eruptions in 2009, 900 in 2010, 600 in 2011 as of September 1, 2011, are classified as explosions with distinct infrasound pressure pulses. Previously, only in 1960, 1974, 1983 and 1985 did the number exceed 400 although it never reached 500.

(3) Several parameters characterizing the intensity of volcanic activity since 2008 were smaller by a factor of 3 to 10 than those during the last active period from 1974 to 1985 (Iguchi *et al.*, 2010). For example, the total weight of ejected volcanic ash in 2009 is estimated to be only 3.2 million tons while in the 1980's it was 10 to 30 million tons every year. In addition, the volumetric changes of the inflation/deflation sources for individual explosions since 2008 were only 10^2 to 10^4 m^3 while those in the 1980's were 10^3 to 10^5 m^3 . Furthermore, the overall seismicity since 2008 was lower than that before 2007; it was not unusual to count more than 2,000 earthquakes per month before 2007 whereas this decreased to less than 800 since 2008.

To summarize, although there have been more frequent explosions since 2008, both the degree of seismicity and

^{*} Earthquake Research Institute, University of Tokyo, 1-1-1, Yayoi, Bunkyo-ku, Tokyo 113-0032, Japan.

^{**} Graduate School of Science, Kyoto University, Kitashirakawa-Oiwakecho, Sakyo-ku, Kyoto 606-8502, Japan.

^{***} Sakurajima Volcano Research Center of Disaster Prevention Research Institute, Kyoto University, 1722-19, Sakurajima-Yokoyama, Kagoshima 891-1419, Japan.

^{****} Key Laboratory of Computational Geodynamics, Graduate University of Chinese Academy of Sciences, 19A Yuquanlu, Beijing 100049, China.

^{*****} Sumiko Consultant Corp., 2-9-7, Ikenohata, Taito-ku, Tokyo 110-0008, Japan.

Table 1. Geographic coordinates of absolute gravity station ARM, Arimura Crustal Deformation Observatory (see also Fig. 1).

Latitude (degree)	Longitude (degree)	Height above mean sea level (meter)	Distance to Showa Crater (meter)
31.56005	130.6724	80	2,100

crustal deformation have been much lower. This strongly suggests that Sakurajima has switched from being a closed-conduit system to an open one as its principal vent changed from Minamidake to Showa crater in 2006. When a volcano's conduit is not tightly plugged for a long period of time, it is expected that mechanical forces associated with the supply of magma rarely build up deep underground; instead, the internal overpressure can easily be relieved by frequent but small-scale explosions. If this is the case, ground deformations and seismicity may no longer be good indicators for diagnosing the volcano. On the other hand, continuous gravity monitoring provides us with information on magma movement in the form of mass transport, particularly when it is not significantly affected by ground uplift/subsidence as is the case for Sakurajima since 2006.

In this paper, we present absolute gravity data from April 2009 through January 2011. We also describe several technical aspects related to carrying out continuous absolute gravity monitoring for more than a year, since this is something that has never been attempted anywhere in the world and so is worth communicating. The absolute gravity records are interpreted in terms of changes in magma head height using a simple line mass model.

2. Absolute Gravity Measurements

The gravity data were obtained using FG5 absolute gravimeters that are installed at the Arimura Crustal Movement Observation Vault, 2.1 km from Showa crater (ARM in Fig. 1, Table 1); three gravimeters (Serial Number #109, #212, and #241) were used in turn to carry out continuous observations without any significant interruptions due to mechanical problems. The acceleration rate of a free falling target was measured every 10 to 15 seconds in a vacuum chamber with a laser interferometer and a rubidium atomic clock (Niebauer *et al.*, 1995; Okubo *et al.*, 1997). The standard deviation for each measurement after correcting for the Earth's tide and the barometric effect was 20 to 50 μgal ($1 \mu\text{gal} = 10^{-6} \text{ cm/sec}^2$), depending on the level of ground noise. Since about 1,200 gravity measurements were performed every day, the error in the daily mean gravity is estimated to be less than $50/(1,200)^{1/2}$, which is $\sim 1 \mu\text{gal}$.

Since absolute gravimeters were originally designed to operate in a clean and quiet laboratory with good temperature control, we faced considerable unexpected problems

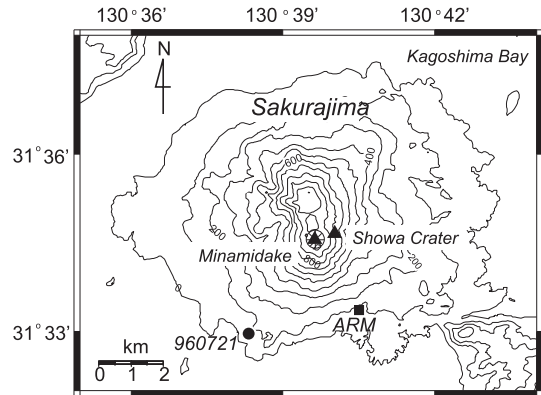


Fig. 1. Location of the ARM absolute gravity station, “Showa Crater” and “Minamidake Crater”. A permanent GPS station of the Geospatial Information Authority of Japan, 960721, is denoted with a solid circle. Contours are drawn every 100 meters above mean sea level.

in operating the FG5 instruments for extended periods of time (Table 2). For example, the laser tube lost power at an unusually fast rate of 25%/month; in ordinary laboratory conditions, the rate is 5%/month or less (Fig. 2). In addition, a personal computer used with the FG5 suffered from frequent abnormal shutdowns a few months after installation. These problems most likely arose due to fine-grained volcanic ash creeping into parts of the gravimeter that were exposed to the open air. After several periods of trial and error, these problems were solved by constructing a vinyl tent around the entire gravimeter; the environment inside then became almost free from volcanic dust (Fig. 3a). The laser tube was treated separately and placed in a compact clean bench (Fig. 3b). These measures to avoid the infiltration of fine dust have been working well since March 2010, and there have consequently been no significant interruptions to the absolute gravity measurements (Table 2).

3. Gravity Changes

Fig. 4 shows the daily means of absolute gravity measured at ARM from April 2009 through January 2011. Unfortunately, the time series is interrupted twice (October 2009 and March 2010) because of unexpected instrumental problems (Table 2). Nevertheless, the data provide us with invaluable information on the mass transport within Sakurajima volcano during the period of most frequent explosions within the last 55 years. We must remember, however, that gravity measurements are also sensitive to mass redistribution just around the observation site. In particular, changes in groundwater level and soil moisture content have a significant influence on local gravity. Consequently, it is crucially important to eliminate these

Table 2. Overview of absolute gravity measurements from April 2009 through January 2011.

Observation Period	Serial #	Number of Daily Measure-ments	Remarks
Apr 10, 2009 – July 11, 2009	#212	1,200	Rapid decrease in laser power (23%/month) during the entire period. Strong variation of 1F voltage (0.1 – 0.4 V) of the iodine stabilized laser from May 18 to June 19. Laser output completely lost from June 19 to June 25. Laser tube was cleaned with alcohol on June 25 to recover the power but the laser was unexpectedly locked to the G and H energy levels of the iodine hyperfine structure.
July 12, 2009 – Sep 13, 2009	#109	600	Rapid decrease in laser power during the entire period. Laser tube was cleaned with alcohol on Aug 31 to recover the power. Yellow-brown stains were found inside the laser tube. Laser output completely lost since Sep 13.
Nov 2, 2009 – Feb 12, 2010	#212	1,200	The gravimeter was installed in a vinyl tent on Nov 2. Data bias of -6.4 μgal from Nov 18 to Nov 26 with unknown origin. The laser tube was placed in a clean bench on Dec 22 to avoid volcanic dust. Frequent abort of measurements due to PC/electronic problems since Dec 23. Cleaning of A/D board on Jan 14 fixed the frequent auto-reboot of the PC. Data bias of -16.5 μgal from Dec 30 to Jan 6 with unknown origin. Data bias of -9.3 to -15.4 μgal from Jan 15 to Jan 21 with unknown origin. Successful measurement rate decreased to <80% since Feb 2, most probably due to the dropper touching the cart. Frequent auto-reboot of the PC since Feb 12.
Feb 25, 2010 – Mar 13, 2010	#241	1,200	Sticky bearing due to abnormally low room temperature.
Mar 30, 2010 – Jan 30, 2011	#109	1,536	

effects from the raw data in order to establish a physical model for magma transport in a volcano.

3-1 Modeling gravity disturbance due to ground-water

Kazama and Okubo (2009) proposed a physical method to estimate the gravity disturbance due to variations in the moisture content $\theta(t)$ of the top unsaturated layer and the water table height $h(t)$. The two variables are governed by

$$\frac{\partial \theta(x,y,z,t)}{\partial t} = \frac{\partial}{\partial z} \left(D_v(\theta;x,y,z) \frac{\partial \theta}{\partial z} + K_v(\theta;x,y,z) \right), \quad (1)$$

$$n(x,y) \frac{\partial h(x,y,t)}{\partial t} = K_{hs}(x,y) \frac{\partial}{\partial x} \left[(h - h_b(x,y)) \frac{\partial h}{\partial x} \right] + K_{hs} \frac{\partial}{\partial y} \left[(h - h_b) \frac{\partial h}{\partial y} \right] + N(x,y,t) \quad (2)$$

where D_v and K_v respectively denote vertical diffusivity and permeability, and n , K_{hs} , h_b , N in the second equation stand for porosity, saturated permeability, height of the upper surface of the impermeable layer, and recharge from the unsaturated layer, respectively. In the following, we assume

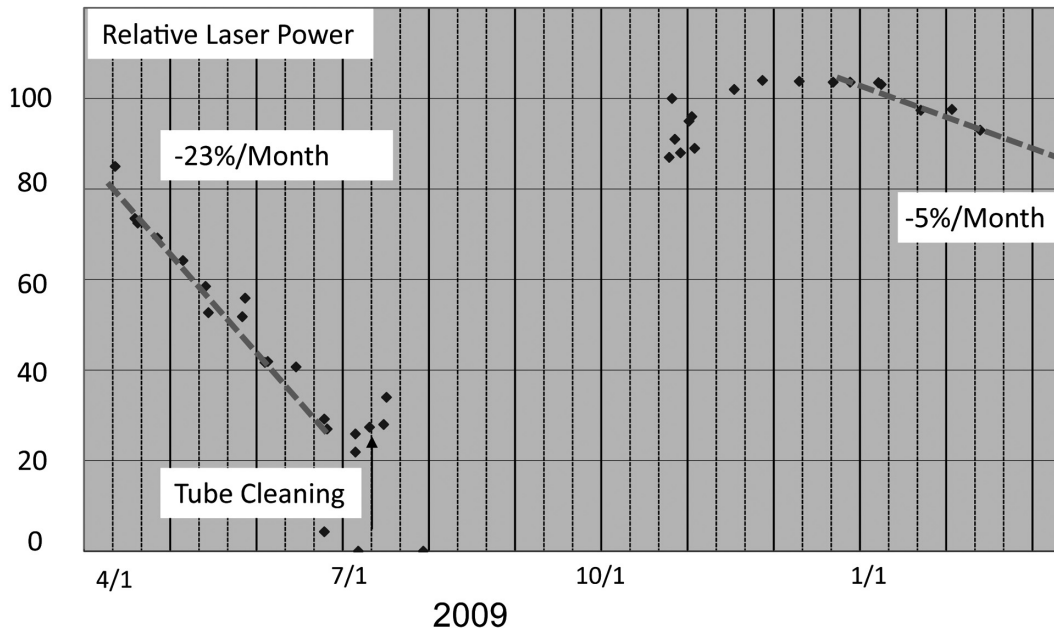


Fig. 2. Laser power as a function of time. Power dropped by about 23 % each month until July 2009. The laser was covered with a clean bench in a vinyl tent in November 2009. Since then, the rate of power loss was restored to the normal value of 5%/month.

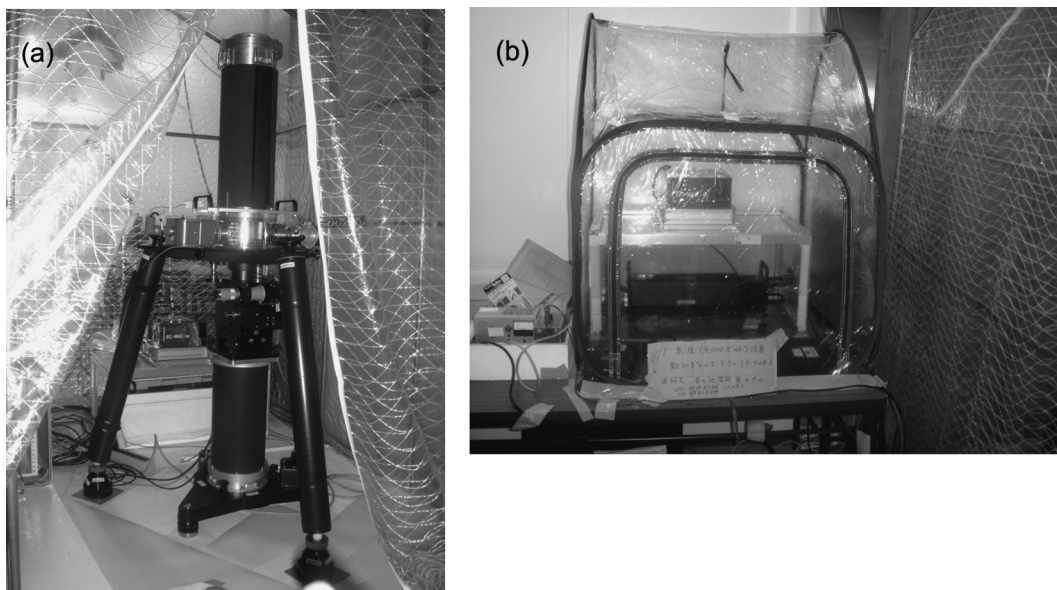


Fig. 3. Protection for the gravimeter against fine-grained volcanic ash. (a) FG5 gravimeter installed in a vinyl tent. (b) The laser was also protected from volcanic ash using a clean bench in a vinyl tent.

$$D_v(\theta;x,y,z) = D_{vs} \exp \left[-b \left(1 - \frac{\theta(x,y,z) - \theta_{\min}}{\theta_{\max} - \theta_{\min}} \right) \right]$$

$$(3) \quad K_v(\theta;x,y,z) = K_{vs} \exp \left[-a \left(1 - \frac{\theta(x,y,z) - \theta_{\min}}{\theta_{\max} - \theta_{\min}} \right) \right], \quad (4)$$

(Gardner and Mayhugh, 1958; Davidson *et al.*, 1969). We take $K_{vs}=5.0 \times 10^{-6}$ m/s, $D_{vs}=1.0 \times 10^{-5}$ m/s, $a=7.98$, $b=1.16$, $\theta_{\min}=0.00$ and $\theta_{\max}=0.50$ as these are representative values for the soil ‘‘Shirasu’’ covering the top surface around Sakurajima (Miwa *et al.*, 1991; Sugio and Okabayashi, 1994; Kazama, 2010). Furthermore, we assume that the porosity $n(x,y)$ and horizontal permeability $K_h(x,y)$ are homogenous in space as

$$n(x,y) = \theta_{\max} = 0.50, \quad (5)$$

$$K_{hs}(x,y) = 3.5 \times 10^{-4} \text{ m/s} \quad (6)$$

based on the averaged data of Oshima (2008). Undulation of h_b is ignored and $h_b(x,y)$ is taken to be -400 m because a low electrical conductivity layer at 400 m below the mean sea level (Kanda *et al.*, 2008) is most likely to be an impermeable layer. Recharge to the saturated layer $N(x,y,t)$ m/s is calculated based on the water content profile at the bottom of the unsaturated layer using the Buckingham-Darcy law (Jury and Horton, 2004), as given by

$$N(x,y,t) = [D_v(x,y,z) + K_v(x,y,z)]_{z=h(t)}. \quad (7)$$

Equations (1)–(2) can be numerically solved for the soil moisture content $\theta(t)$ and the water table height $h(t)$ under appropriate initial and boundary conditions using the Finite Difference Method (FDM). In our FDM computations, vertical and horizontal grid sizes are set at $\Delta z=1.0$ m, $\Delta x=59.3$ m (east-west) and $\Delta y=46.3$ m (north-south), which match those of the digital elevation model of the Geographical Survey Institute (1997).

The boundary conditions are the same as those described in Kazama (2010). We take

$$\left[D_v \frac{\partial \theta}{\partial z} + K_v \right]_{z=h_g(x,y)} = R(t) - E(t), \quad (8)$$

$$\left[D_v \frac{\partial \theta}{\partial z} + K_v \right]_{z=h(t)} = 0, \quad (9)$$

$$\theta(x,y,h(t),t) = \theta_{\max} = n, \quad (10)$$

$$h(x_{coast}, y_{coast}, t) = 0, \quad (11)$$

$$K_{hs} \left(\frac{\partial h}{\partial x} e_x + \frac{\partial h}{\partial y} e_y \right)_{(x_d, y_d)} = 0 \quad (12)$$

where $h_g(x,y)$ represents undulations of the ground as obtained from digital elevation models (Geographical Survey Institute, 1997). $R(t)$ is the precipitation measured using a rain gauge while $E(t)$ denotes the evapotranspiration estimated from daily means of surface temperature, relative humidity, wind speed and hours of sunshine (Penman, 1948). (x_{coast}, y_{coast}) and (x_d, y_d) represent the horizontal coordinates of seacoast and water divides around the target area while e_x and e_y are the horizontal

components of the vector normal to the water divide.

In brief, Eqs. (8)–(9) are derived by considering the vertical soil-water flux on the ground and at the top of the shallowest impermeable layer (*i.e.*, bottom of saturated layer). Equation (10) is obtained based on the fact that the soil at the interface of the saturated/unsaturated layers must be saturated with water. Equation (11) specifies that the sea level should match the water table along the coast, while Eq. (12) implies that groundwater does not flow across the water divide.

The initial conditions for the soil moisture content $\theta(t)$ and the water table height $h(t)$ are obtained in the following manner. We first derived steady state solutions to Eqs. (1)–(2) by carrying out an FDM simulation with *arbitrary* initial conditions and with boundary conditions (8)–(12), with annual mean values substituted for $R(t)$ and $E(t)$. Whatever the initial conditions, the FDM solution converges to a steady state solution within 500 years. We then carried out an FDM simulation again using real data for $R(t)$ and $E(t)$ obtained since January 2006 as the boundary conditions and using the steady state as the initial conditions. The FDM results for January 1, 2009 can be used as the initial conditions; a two-year run-up computation is usually sufficient to suppress transient fake solutions.

Once the soil moisture content $\theta(t)$ and the water table height $h(t)$ are obtained by the FDM simulation, it is straightforward to estimate the gravity disturbance $g_w(t)$ at a given station (x_0, y_0, z_0) as the sum of g_1 and g_2 , which represent hydrological gravity effects arising from the unsaturated and saturated layers, respectively.

$$\begin{aligned} g_w(x_0, y_0, z_0, t) &= g_1(x_0, y_0, z_0, t) + g_2(x_0, y_0, z_0, t), \\ g_1(x_0, y_0, z_0, t) &= -G\rho_w \iint \left(\int_{h_b(x,y,t)}^{h_g(x,y)} \theta(x,y,z,t) \frac{z-z_0}{r^3} dz \right) dx dy, \\ g_2(x_0, y_0, z_0, t) &= -G\rho_w \iint n(x,y) \left(\int_{h_b(x,y)}^{h(x,y,t)} \frac{z-z_0}{r^3} dz \right) dx dy, \end{aligned} \quad (13)$$

$$r = \sqrt{(x-x_0)^2 + (y-y_0)^2 + (z-z_0)^2}$$

where G , ρ_w , and h_s are the gravitational constant, water density, and ground surface elevation, respectively.

Fig. 4 presents the absolute gravity change before and after correcting for the hydrological disturbance. It can be clearly observed that the peak-to-peak fluctuation is reduced from 30 μgal to 15 μgal once the groundwater correction is applied to the raw data. In general, however, a small fluctuation does not necessarily guarantee that the correction is adequately performed. We may, however, certainly say that a significant part of the ground water disturbance is successfully eliminated because the same formulation gave excellent agreement between the observed and

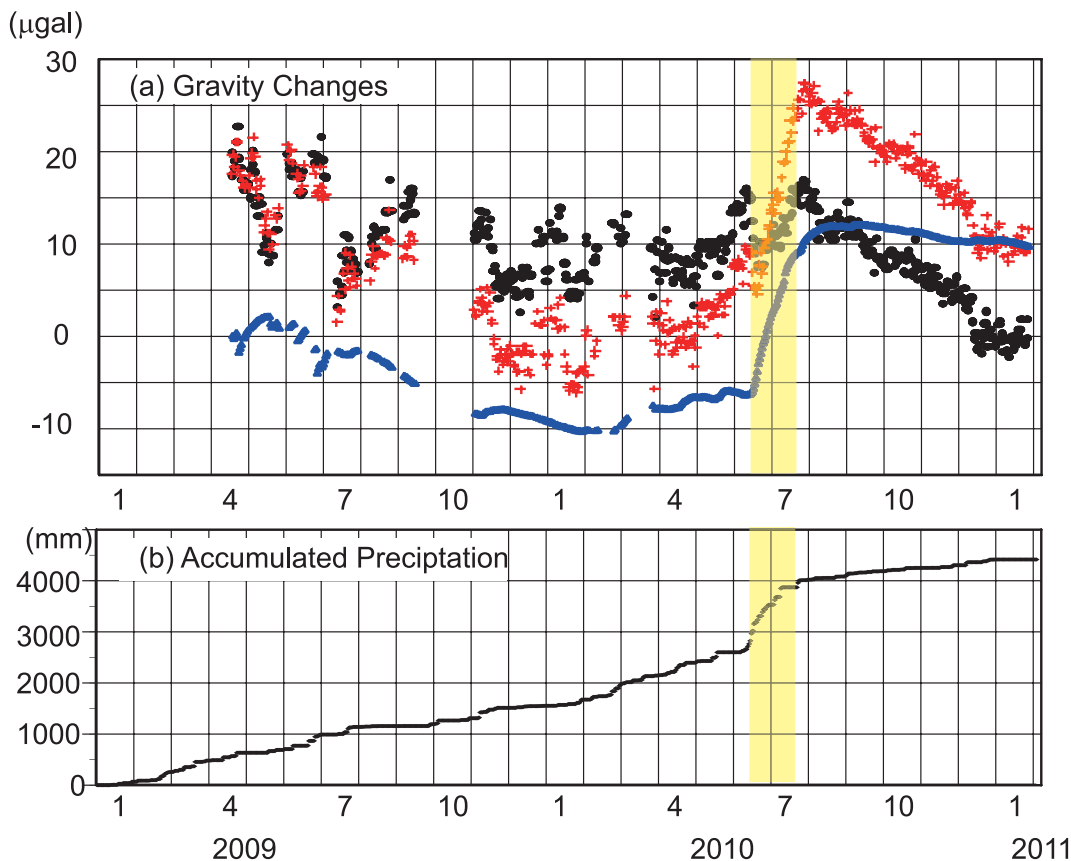


Fig. 4. Gravity and precipitation.
 (a) Gravity changes at ARM (Fig. 1) from March 2009 through January 2011. Red crosses and blue circles denote raw gravity data after subtracting a nominal value of 979,437,796 μgal and the estimated groundwater disturbance, respectively. Gravity after eliminating the groundwater disturbance is indicated by black circles.
 (b) Accumulated precipitation at ARM since January 1, 2009. During the period shaded in yellow, a large error might be present in the estimate of the groundwater disturbance owing to unusually heavy rainfall (more than 1,000 mm in a month).

computed soil moisture content $\theta(t)$ (Kazama 2010).

One point is worth noting concerning the correction during the heavy rainfall period, *i.e.*, from the middle of June 2010 to the end of July 2010 (Fig. 4). In Fig. 4, a rather unnatural bump is visible during that period. We believe this is due to the shortcomings of our hydrological model for the period in question. Equations (1) and (2) may not fully represent actual hydrological processes in unusual circumstances. In fact, precipitation during this period totaled 1,500 mm, three times larger than the rainfall during the same season in 2009. It is therefore likely that gravity remained almost unchanged if the groundwater effect was eliminated.

3-2 Gravity Change as an Indicator of Volcanic Activity

It is worthwhile reviewing the volcanic activity that

occurred during the period of our gravity measurements. For this purpose, we show the ejected weight of volcanic ash, ground tilt, and infrasound impulse amplitude as functions of time in Fig. 5. It is clearly seen in Fig. 5(a), (b) and (d) that the entire period (from January 2009 to the end of January 2011) is divided into five phases, namely phase I to V. This division agrees in principle with Iguchi *et al.* (2011a), who divided the same period into 4 phases; they actually divided the period after September 30, 2009, into 3 phases.

Phase I lasted until the end of June 2009 without any significant ejection of volcanic ash. It was followed by phase II (inflation period of Iguchi *et al.* (2011)) when explosive eruptions began to occur frequently, accompanied by a remarkable increase in the volume of ejected volcanic ash. Phase III (from early May 2010 to the middle

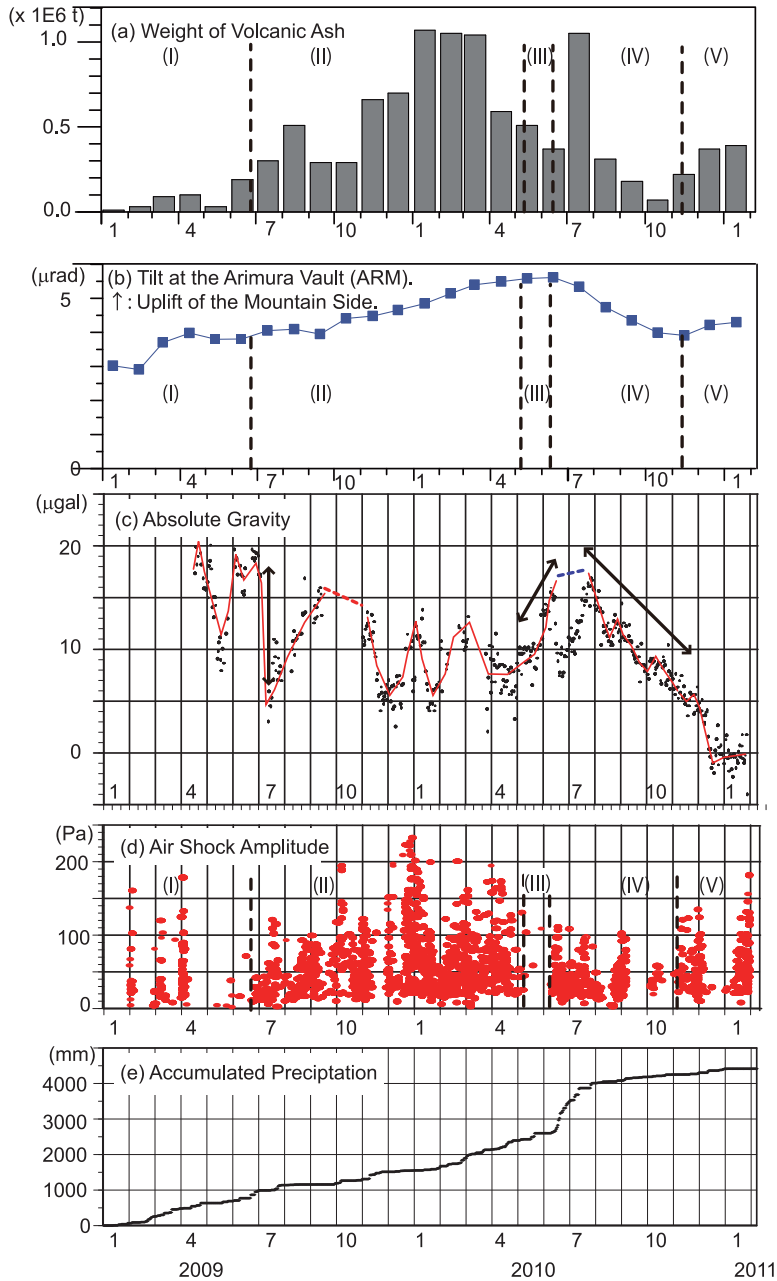


Fig. 5. Gravity change (after eliminating the groundwater disturbance) compared with indices of volcanic activity. The entire period is divided into 5 phases (I to V) based on the volcanic activity. (a) Weight of volcanic ash ejected each month (Iguchi *et al.*, 2013). (b) Ground tilt toward the center of Showa crater (Iguchi *et al.*, 2011). (c) Absolute gravity variation at ARM with correction for groundwater disturbance. Black circles are daily means while the red curve and the blue dotted line represent the smoothed gravity variation allowing for a probable overcorrection in June and July, 2010. (d) Infrasound impulse amplitude at a microphone site around Arimura (Iguchi *et al.*, 2013). (e) Accumulated precipitation since January 1, 2009.

of June 2010) can be identified as a short but distinctive quiescent period with few explosions. It is likely to be a transient period because it was followed by phase IV (deflation period of Iguchi *et al.*, (2011)), characterized by significant deflation of the volcano, which strongly suggests a decrease in the supply of magma deep underground. Phase IV lasted until the middle of November 2010. Since then, volcanic activity has been in phase V (re-inflation period of Iguchi *et al.*, (2011)) and all of the indices have been gradually restored to their phase II levels.

The gravity changes at ARM, following correction for groundwater effects (Fig. 5(c)), are compared with the three volcanic indices in Figs. 5(a), (b), and (d). We would like to draw attention to the following points:

- (1) Gravity decreased very rapidly (*ca.* 20 $\mu\text{gal}/\text{month}$) during a short transition interval from phase I to the more active phase II.
- (2) Gravity oscillated about a mean value with an amplitude of *ca.* 5 μgal during phase II.
- (3) Gravity increased rapidly (*ca.* 5 $\mu\text{gal}/\text{month}$) during the short transient phase III.
- (4) Gravity decreased steadily during phase IV.
- (5) Gravity ceased to decrease during phase V.

The above observations strongly suggest that movement of magma in the conduit of Showa crater is reflected in specific gravity changes.

4. Estimating Magma Head Height from Gravity Change

The elevation around ARM during our observational period remained almost unchanged, with a random observational noise of 1 cm or so according to the F3 solution¹ of the nearest permanent GPS station 960721 of the Geospatial Information Authority of Japan (Fig. 1). The rather insignificant amount of crustal deformation despite the frequent Vulcanian eruptions in 2009 and 2010 (Fig. 5) implies that overpressure in the magma chamber was not effectively transmitted to the surrounding medium. In other words, it is very likely that Sakurajima volcano was erupting as an open conduit system during our observational period. Even if we were to take 2 cm as the elevation change at ARM during our observation period, its effect on the gravity is still only about 4 to 6 μgal , depending on the choice of the Free Air or Bouguer gravity gradient. Since this is smaller than the observed 20 μgal gravity change by a factor of 3 to 5 (Fig. 5), we are left with two possibilities to explain the observed gravity change: (1) temporal variation of mass in a magma reservoir, or (2) movement of magma head in the conduit. Ishihara (1990) and Iguchi *et al.* (2013) argued that there are two principal magma reservoirs: a deeper one located at 10 km depth beneath the center of Aira caldera (~ 10 km

north of Sakurajima) and a shallower one at 2–6 km depth below Minamidake crater (Fig. 1). Gravity changes due to mass increases at these reservoirs, without crustal deformation occurring, are estimated to be 3 to 10 $\mu\text{gal}/\text{year}$ if we take $10^7 \text{ m}^3/\text{year}$ as a reasonable magma supply rate (Ishihara 1990, Iguchi *et al.* 2013). Since these rates are an order of magnitude smaller than the observed rate of *ca.* 10 $\mu\text{gal}/\text{month}$ (Fig. 4), we conclude that temporal variation of mass in a magma reservoir is not a major source of the observed gravity variation. In the following, we investigate whether the observed gravity change can be well explained in terms of variation of the magma head height, similar to the approach taken by Okubo (2005) for Asama volcano.

Let us first assume the conduit to be a vertical cylinder in which rock fragments and/or solidified magma form a porous matrix with a porosity ϕ , as shown in Fig. 6(a). A melt with a density ρ_{melt} is assumed to rise and fall within the conduit through the matrix. Since the diameter a of the conduit (~ 100 m) is much smaller than the horizontal distance L ($=2,100$ m) between the conduit and the ARM observation point, the attraction Δg due to the magma column should be well represented by that of a line mass as

$$\Delta g(H(t)) = \pi G a^2 \rho_{\text{melt}} \phi \left(\frac{1}{\sqrt{L^2 + (H(t) - H_0)^2}} - \frac{1}{L} \right) + \Delta g_0$$

$$\Delta g_0 \equiv \Delta g(H(t) = H_0) \quad (14)$$

where G is the gravitational constant, $H(t)$ is the height of the magma head above mean sea level (MSL) at a time t , and H_0 is the height of the gravity station (Fig. 6(a)). We may solve Eq. (14) for $H(t)$ in terms of $\Delta g(t)$ as

$$H(t) = H_0 \pm L \sqrt{\left(\frac{G\sigma}{G\sigma + (\Delta g(t) - \Delta g_0)L} \right)^2 - 1} \quad (15)$$

$$\sigma \equiv \pi a^2 \rho_{\text{melt}} \phi$$

We should be aware here that Eq. (15), which links Δg to variations in H , is not single valued. We may, however, resolve this ambiguity by remembering that $H(t)$ is a continuous function of time and by choosing an appropriate initial condition. By substituting $L = 2,100$ m, $H_0 = 80$ m (Table 1) into Eq. (15), and assuming the physically plausible values $\rho_{\text{melt}} = 2.67 \times 10^3 \text{ kg}/\text{m}^3$, $a = 100$ m, and $\phi = 0.75$, we can determine the height of the magma head as a function of time (Fig. 6(b)). As an initial condition, we assumed $H_0 = 80$ m (*i.e.*, the height of the gravity station) in June 2009 when the gravity was a maximum.

Fig. 6(b) shows the following interesting features. The magma head was 400–800 m above the MSL during the most active phase II, which is quite high in the conduit because the elevation of Showa crater is *ca.* 800 m (Fig. 1). Phase III is characterized by a sudden fall of the head from 800 m to 0 m, implying temporary weakening of the driving pressure in the conduit. This is consistent with the 1 month quiescent period with few explosions. Phase IV is characterized by a steady fall in magma level, which is

¹ <http://terras.gsi.go.jp/ja/index2.php>

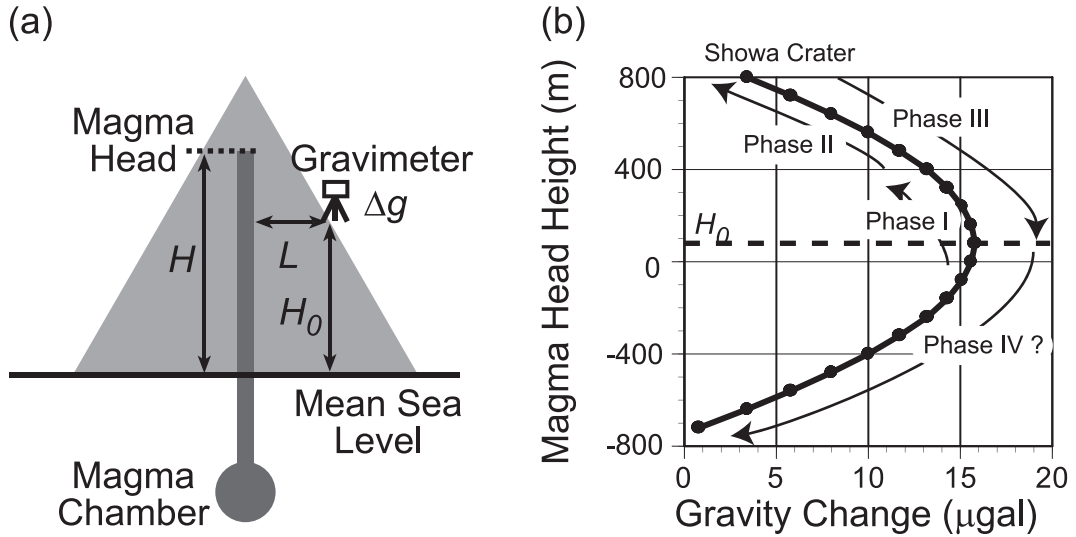


Fig. 6. Method of estimating height of the magma head in the conduit. (a) Line mass model used to calculate the elevation of the magma head. A gravimeter is installed at an elevation H_0 above mean sea level. The distance from the conduit to the gravimeter is L . (b) Magma head height $H(t)$ derived from gravity change $\Delta g(t)$ using Eq. (15). Phases I to IV (?) correspond to those in Fig. 5.

consistent with the deflation of Sakurajima volcano (Iguchi 2011). It should be noted, however, that systematic bias might have been introduced into the data since July 2010 by a significant ground water disturbance during June–July 2010 (Fig. 4). If the gravity in phase IV is biased by -5 to $-10 \mu\text{gal}$, the estimated magma head height includes an error of a few hundred meters.

5. Conclusions and Discussion

We carried out absolute gravity measurements for 21 months from April 2009 through January 2011 at Sakurajima volcano, paying special attention to avoid interruptions to the record. The gravity exhibited characteristic variations associated with 5 distinct phases linked to the volcanic activity. The absence of any significant elevation change at the gravity station enabled us to infer the magma head height by using a simple line mass model. The estimated height until July 2010 is consistent with the eruptive activity of Showa crater while that after August 2010 might be biased by our possibly inappropriate hydrological model. We should be also aware that several assumptions used in the modeling must be justified in future studies, including the conduit radius and the porosity. However, our estimates of the fluctuations in the magma head height can serve as a basis or a working hypothesis to better understand the eruptive activity of Showa crater of Sakurajima volcano.

Acknowledgments

We express our sincere thanks to the Osumi Office of

River and National Highway, Kyushu Regional Development Bureau, Ministry of Land, Infrastructure, Transport and Tourism for allowing us to use the facilities of the Arimura Crustal Deformation Observation Vault and providing us with hourly precipitation data. Special thanks are given to members of the Sakurajima Volcano Observatory, Kyoto University for providing us with technical support to continue our research. We appreciate discussion with the members of the Institute of Physical Geodesy, Technical University of Darmstadt during the first author's stay in Germany, supported by the Alexander von Humboldt Foundation. This work was supported in part by a Grant-in-Aid for Scientific Research (20244071) and in part by the Collaborative Research Program of the Disaster Prevention Research Institute, Kyoto University (21G-04, 22G-07).

References

- Davidson, J. M., Stone, L. R., Nielsen, D. R. and Larue, M. E. (1969) Field measurement and use of soil-water properties. *Water Resour. Res.*, **5** (6), 1312–1321.
- Gardner, W. R. and Mayhugh, M. S. (1958) Solutions and tests of the diffusion equation for the movement of water in soil. *Soil Sci. Soc. Am. Proc.*, **22**, 197–201.
- Geographical Survey Institute (1997) Suuchi chizu 50 m mesh (Hyoukou) Nippon III [CD-ROM]. Japan Map Center, Tokyo, Japan.
- Iguchi, M. (2011) Volcanic activity and prediction of volcanic eruption by using ground deformation data in underground tunnels at Sakurajima volcano, Japan. *Abstract of the Sym-*

- posium on Prediction of Eruption at Volcanoes under Open-conduit*, July 14, 2011, Kagoshima, Japan (in Japanese).
- Iguchi, M., Yokoo, A. and Tameguri, T. (2010) Intensity of volcanic explosions at Showa Crater of Sakurajima Volcano. *Annals Disas. Prev. Res. Inst., Kyoto Univ.*, **53B**, 233-240 (in Japanese with English abstract).
- Iguchi, M., Ohta, Y., Ueki, S., Tameguri, T., Sonoda, T., Takayama, T. and Ichikawa, N. (2011) Evaluation of volcanic activity of Sakurajima volcano in 2010. *Annals Disas. Prev. Res. Inst., Kyoto Univ.*, **54B**, 171-183 (in Japanese with English abstract).
- Iguchi, M., Tameguri, T., Ohta, Y., Ueki, S. and Nakao, S. (2013) Characteristics of volcanic activity at Sakurajima volcano's Showa crater during the period 2006 to 2011. *Bull. Volcanol. Soc. Japan*, **58**, 115-135.
- Ishihara, K. (1990) Pressure sources and induced ground deformation associated with explosive Eruptions at an andesitic volcano: Sakurajima volcano, Japan. In *Magma Transport and Storage* (M.P. Ryan, ed.), John Wiley and Sons, 335-356.
- Jury, W. A. and Horton, R. (2004) *Soil Physics*. 6th ed., John Wiley, Hoboken, N. J. 370 p.
- Kanda, W. *et al.* (2008) AMT electrical resistivity survey at Sakurajima volcano. In *Report on the 10-th integrated observation campaign of Sakurajima volcano*, issued by Sakurajima Volcano Res. Center, Disas. Prev. Res. Inst., Kyoto Univ., 89-104 (in Japanese).
- Kazama, T. (2010) Hydrological modeling of groundwater disturbances to observed gravity data toward high-accuracy monitoring of magma transfer in volcanoes. Ph.D thesis, University of Tokyo, pp. 196 (in Japanese with English abstract).
- Kazama, T. and Okubo, S. (2009) Hydrological modeling of groundwater disturbances to observed gravity: theory and application to Asama volcano, central Japan. *J. Geophys. Res.*, **114**, B08402, doi: 10.1029/2009JB006391.
- Miwa, K., Nanba, N., and Wakumatsu, C. (1991) Measurement of unsaturated hydraulic conductivity of mixed soil: wetting process. *Bull. Fac. Agric. Kagoshima Univ.*, **41**, 81-87 (in Japanese with English abstract).
- Niebauer, T. M., Sasagawa, G. S., Faller, J. E., Hilt, R. and Klotting, F. (1995) A new generation of absolute gravimeters. *Metrologia*, **32**, 159-180.
- Okubo, S. (2005) Gravity changes associated with volcanism-observation, theory, and analysis. *Bull. Volcanol. Soc. Japan*, **50**, S49-S58 (in Japanese with English Abstract).
- Okubo, S., Yoshida, S., Sato, T., Tamura, Y. and Imanishi, Y. (1997) Verifying the precision of a new generation absolute gravimeter FG5-comparison with superconducting gravimeters and detection of oceanic loading tide. *Geophys. Res. Lett.*, **24**, 489-492 doi: 10.1029/97GL00217.
- Oshima, H. (2008) Groundwater in the shallow part of Sakurajima volcano-archived data. In *Report on the 10-th integrated observation campaign of Sakurajima volcano*, issued by Sakurajima Volcano Res. Center, Disas. Prev. Res. Inst., Kyoto Univ., 191-193 (in Japanese).
- Penman, H. L. (1948) Natural evaporation from open water, bare soil and grass. *Proc. Roy. Soc. Lond. Ser. A*, **193**, 120-145.

(Editorial handling Takeshi Nishimura)

2009年4月～2011年1月の桜島火山における絶対重力観測 —昭和火口からの噴火活動に関する考察

大久保修平・風間卓仁・山本圭吾・井口正人・田中愛幸・菅野貴之・
今西祐一・孫 文科・坂 守・渡邊篤志・松本滋夫

2009年4月から2011年1月まで、桜島火山の有村観測坑で行った絶対重力の連続観測により、測定誤差を有意に超える、30マイクロガルの重力値の減少が検出された。陸水流動シミュレーションを用いて、降雨等により発生する地下水起源の重力擾乱を取り除くと、重力は両振幅で15～20マイクロガルの変動を示した。変動の様相から観測期間が5つの特徴的なフェーズに分けられることが明らかとなった。これらのフェーズは、火山灰放出量・有村における傾斜変動・爆発回数などの火山活動を示す指標の変動と、きわめて良い相関をもっていた。重力の火道内のマグマ頭位の変動によって重力変動が引き起こされると考え、線質量モデルに基づいて、頭位標高の推移を推定した。その結果から、マグマヘッドは2009年7月～2010年5月半ばには標高400～800mと高い位置にあったが、その後の1か月間で標高0m程度まで急降下していると推定された。これらの推定は、昭和火口からの爆発回数の消長ときわめて良い対応を見せている。